Electronic supplementary information

Contents

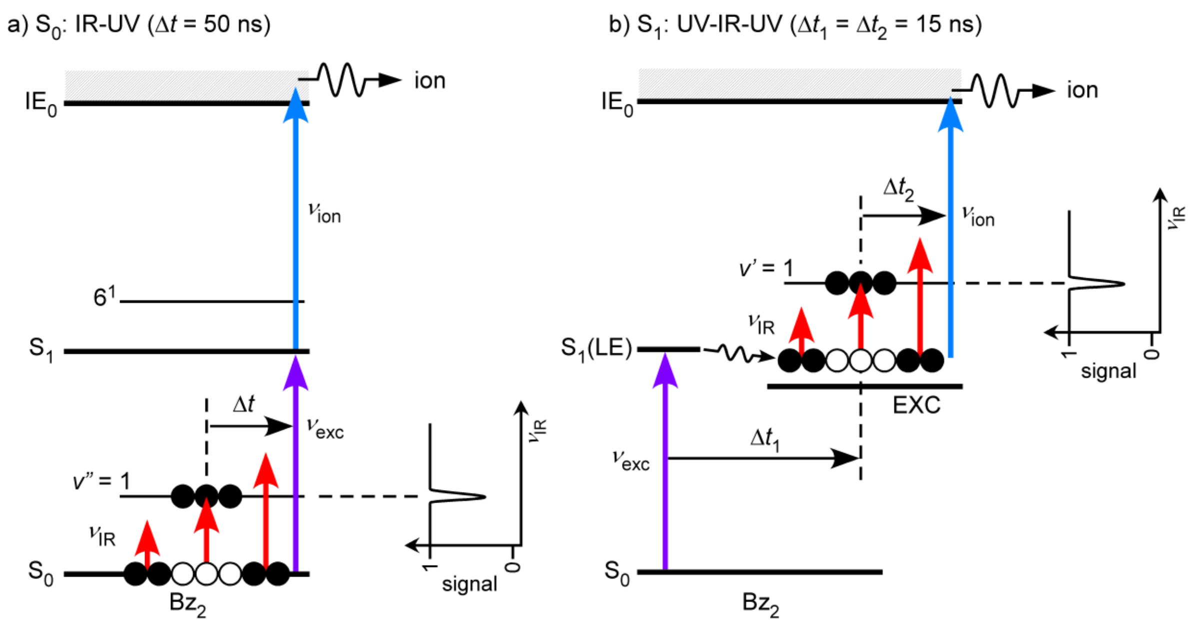

Figure S1 Excitation schemes of (a) IR-UV spectroscopy for a S_0 state and (b) UV-IR-UV spectroscopy for a S_1 state. In this work, ν_{IR} was fired 50 ns prior to the two UV pulses (Δt = 50 ns) for the IR-UV spectroscopy, while ν_{IR} was irradiated 15 ns after ν_{exc}, and ν_{ion} was fired 15 ns after ν_{IR} ($\Delta t_1 = \Delta t_2$ = 15 ns) for the UV-IR-UV spectroscopy according to the lifetime of the S_1 state of Bz_2 (~40 ns).[64] ν_{ion} was set to 270 nm for Bz and 285 nm for Bz_2, respectively.

Table S1 Comparison of C–C bond lengths in Bz ($r_{C–C}$), distances between centers of each Bz ring ($r_{Bz\text{-}Bz}$), binding energies of EXC (D_0) of benzene (Bz) and benzene dimer (Bz_2) obtained by (TD-)M06-2X/cc-pVDZ and (TD-)CAM-B3LYP/aug-cc-pVTZ with GD3BJ empirical dispersion correction levels of theory. Upper and lower rows of each parameter show results by M06-2X and CAM-B3LYP functionals, respectively. $r_{Bz\text{-}Bz}$ means distance between centers of each Bz ring.

	Bz (S_0)	Bz (S_1)	Bz_2 (EXC, SW, D_{6h})	Bz_2 (S_1(stem*), T, C_{2v})
$r_{C–C}$ / pm	139.5	142.5	140.8	142.5 (stem); 139.5 (top)
	138.5	141.5	139.8	141.4 (stem); 138.5 (top)
$r_{Bz\text{-}Bz}$ / pm			299.8	488.2
			304.7	496.4
D_0 / cm^{-1}			4428	641
			4113	845

Table S2 Theoretical (ν_{calc}) vibrational frequencies and the assignments of Bz and Bz_2 in the S_0 and S_1 states calculated by normal mode analyses on the optimized structures obtained by M06-2X/cc-pVDZ and TD-M06-2X/cc-pVDZ level of theory, respectively.

[a] These are scaled values by 0.98 for skeletal vibrations and 0.95 for CH stretching vibrations, respectively. Values in parentheses are transition intensities in km/mol.

[b] +/− on the shoulder means the signs of the linear combinations, see text. Symmetry species in the D_{6h} point group are denoted in parentheses.

Bz (S_0)		Bz (S_1)		Bz_2 (S_1, SW, D_{6h})		Bz_2 (S_1, T, C_{2v})	
ν_{calc} / cm^{-1} [a]	assignments[b]	ν_{calc} / cm^{-1} [a]	assignments	ν_{calc} / cm^{-1} [a]	assignments[b]	ν_{calc} / cm^{-1} [a]	assignments
				66 (0)	R_z	−26 (0)	R_y
				104 (0)	$\beta_{(x, y)}$	−9 (0)	R_x
				104 (0)	$\beta_{(x, y)}$	13 (0)	R_z
				118 (0.14)	$R_{(x, y)}$	70 (0)	σ_z
				118 (0.14)	$R_{(x, y)}$	88 (0)	β_x
				152 (0)	σ_z	90 (0)	β_y
404 (0)	16 (e_{2u})	244 (0)	16	348 (0)	16^- (e_{2g})	241 (0)	16a (stem)
				366 (0)	16^+ (e_{2u})	251 (0)	16b (stem)
		253 (0)	4			262 (0)	4 (stem)
						402 (0)	16b (top)
602 (0)	6 (e_{2g})			512 (0)	6^+ (e_{2g})	403 (0)	16a (top)
		508 (0)	6	576 (0)	6^- (e_{2u})	505 (0)	6b (stem)
						514 (0)	6a (stem)
						549 (93)	11 (stem)
712 (0)	4 (b_{2g})			577 (0)	4^- (b_{1u})	561 (0)	10a (stem)
				596 (0)	4^+ (b_{2g})	585 (0)	10b (stem)
678 (92)	11 (a_{2u})	553 (119)	11	625 (83)	11^+ (a_{2u})	601 (0)	6a (top)
				643 (0)	11^- (a_{1g})	601 (0)	6b (top)
858 (0)	10 (e_{1g})	576 (0)	10	749 (0)	10^+ (e_{1g})	681 (108)	11 (top)
				751 (7.2)	10^- (e_{1u})	708 (0)	4 (top)
						752 (0)	17a (stem)
						777 (0)	17b (stem)
981 (0)	17 (e_{2u})	765 (0)	17	875 (0)	17^- (e_{2g})	809 (0)	5 (stem)
				881 (0)	17^+ (e_{2u})	859 (0)	10a (top)
						863 (0)	10b (top)
						964 (1)	1 (stem)
1012 (0)	5 (b_{2g})	807 (0)	5	900 (0)	5^- (b_{1u})	969 (1)	12 (stem)
				914 (0)	5^+ (b_{2g})	974 (1)	18a (stem)
1018 (0)	1 (a_{1g})	963 (0)	1	914 (38)	1^- (a_{2u})	977 (3)	18b (stem)
987 (0)	12 (b_{1u})	963 (0)	12	978 (0)	12^- (b_{2g})	982 (0)	17a (top)

				979 (0)	12^{+} (b_{1u})	985 (0)	17b (top)
				993 (0)	1^{+} (a_{1g})	987 (0)	12 (top)
1048 (10)	18 (e_{1u})	976 (6)	18	1014 (8.6)	18^{+} (e_{1u})	1012 (0)	5 (top)
				1017 (0)	18^{-} (e_{1g})	1015 (0)	1 (top)
						1047 (4)	18a (top)
						1048 (5)	18b (top)
1129 (0)	15 (b_{2u})	1132 (0)	15	1132 (0)	15^{-} (b_{1g})	1128 (1)	15 (stem)
				1135 (0)	15^{+} (b_{2u})	1131 (0)	15 (top)
1162 (0)	9 (e_{2g})	1146 (0)	9	1135 (0)	9^{-} (e_{2u})	1139 (1)	9a (stem)
				1155 (0)	9^{+} (e_{2g})	1147 (2)	9b (stem)
						1161 (0)	9a (top)
						1164 (0)	9b (top)
1330 (0)	3 (a_{2g})	1315 (0)	3	1321 (0)	3^{-} (a_{1u})	1312 (0)	3 (stem)
				1321 (0)	3^{+} (a_{2g})	1327 (0)	14 (top)
1326 (0)	14 (b_{2u})	1573 (0)	14	1435 (0)	14^{+} (b_{2u})	1331 (0)	3 (top)
1486 (18)	19 (e_{1u})	1420 (14)	19	1449 (44)	19^{+} (e_{1u})	1415 (12)	19a (stem)
				1453 (0)	19^{-} (e_{1g})	1420 (5)	19b (stem)
						1484 (10)	19a (top)
						1486 (9)	19b (top)
				1454 (0)	14^{-} (b_{1g})	1572 (1)	14 (stem)
1649 (0)	8 (e_{2g})	1583 (0)	8	1541 (0)	8^{-} (e_{2u})	1582 (0)	8b (stem)
				1615 (0)	8^{+} (e_{2g})	1582 (0)	8a (stem)
						1644 (0)	8b (top)
						1645 (0)	8a (top)
3039 (0)	13 (b_{1u})	3064 (0)	13	3047 (0)	13^{-} (b_{2g})	3042 (0)	13 (top)
				3048 (0)	13^{+} (b_{1u})	3050 (0)	7b (top)
3048 (0)	7 (e_{2g})	3068 (0)	7	3052 (0)	7^{+} (e_{2g})	3053 (0)	7a (top)
				3055 (0)	7^{-} (e_{2u})	3061 (0)	13 (stem)
						3063 (0)	7b (stem)
						3064 (18)	20b (top)
3063 (52)	20 (e_{1u})	3084 (34)	20	3070 (0)	20^{-} (e_{1g})	3067 (18)	20a (top)
				3071 (68)	20^{+} (e_{1u})	3070 (13)	7a (stem)
						3075 (0)	2 (top)
						3079 (18)	20b (stem)
3072 (0)	2 (a_{1g})	3094 (0)	2	3076 (32)	2^{-} (a_{2u})	3087 (5)	20a (stem)
				3082 (0)	2^{+} (a_{1g})	3115 (3)	2 (stem)

Table S3 Comparison between the theoretical average frequencies of the S_0 and S_1 states (ν_{ave}) and the EXC state (ν_{EXC}) calculated at M06-2X/cc-pVDZ and TD-M06-2X/cc-pVDZ level of theory with GD3BJ empirical dispersion correction, respectively. The second column lists frequencies in the EXC state, ν_{EXC}, and absolute values of splitting of the modes, $|\Delta\nu_{EXC}(+/-)| = |\nu_{EXC}(+) - \nu_{EXC}(-)|$, and percentage of the splitting to the average frequencies $\langle\nu_{EXC}\rangle = (\nu_{EXC}(+) + \nu_{EXC}(-))/2$. The third column shows deviations from the average values ($\Delta\nu = \nu_{EXC} - \nu_{ave}$) and percentages of difference to the average values.

Mode	ν_{ave} / cm^{-1} ($\nu(S_0)$; $\nu(S_1)$; $\Delta\nu(S_1/S_0)$)	ν_{EXC} / cm^{-1} ($|\Delta\nu_{EXC}(+/-)|$; $|\Delta\nu_{EXC}(+/-)|/\langle\nu_{EXC}\rangle$)	$\Delta\nu$ / cm^{-1} ($\Delta\nu$ / ν_{ave})
ν_{16} (e_{2u}; op)	324 (404; 244; −160)	241(−), 251(+) (10; 4.1 %)	−83, −73 (−26 %, −23 %)
ν_{6} (e_{2g}; ip)	555 (602; 508; −94)	512(+), 576(−) (64; 12 %)	−43, −21 (−7.7 %, −3.8 %)
ν_{4} (b_{2g}; op)	483 (712; 253; −459)	577(−), 596(+) (19; 3.2 %)	+94, +113 (+19 %, +23 %)
ν_{11} (a_{2u}; op)	616 (678; 553; −135)	625(+), 643(−) (18; 2.8 %)	+9, +27 (+1.5 %, +4.4 %)
ν_{10} (e_{1g}; op)	717 (858; 576; −282)	749(+), 751(−) (2; 0.3 %)	+32, +34 (+4.5 %, +4.7 %)
ν_{17} (e_{2u}; op)	873 (981; 765; −216)	875(−), 881(+) (6; 0.7 %)	+2, +8 (+0.2 %, +0.9 %)
ν_{5} (b_{2g}; op)	910 (1012; 807; −205)	900(−), 914(+) (14; 1.5 %)	−10, +4 (−1.1 %, +0.4 %)
ν_{1} (a_{1g}; ip)	991 (1018; 963; −55)	914(−), 993(+) (79; 8.3 %)	−77, +2 (−7.8 %, +0.2 %)
ν_{12} (b_{1u}; ip)	975 (987; 963; −24)	978(−), 979(+) (1; 0.1 %)	+3, +4 (+0.3 %, +0.4 %)
ν_{18} (e_{1u}; ip)	1012 (1048; 976; −72)	1014(+), 1017(−) (3; 0.3 %)	+2, +5 (+0.2 %, +0.5 %)
ν_{15} (b_{2u}; ip)	1131 (1129; 1132; +3)	1132(−), 1135(+) (3; 0.3 %)	+1, +4 (+0.1 %, +0.4 %)
ν_{9} (e_{2g}; ip)	1154 (1162; 1146; −16)	1135(−), 1155(+) (20; 1.7 %)	−7, +13 (−0.4 %, +0.7 %)
ν_{3} (a_{2g}; ip)	1323 (1330; 1315; −15)	1321(−), 1321(+) (0; 0 %)	−2, −2 (−0.2 %, −0.2 %)
ν_{14} (b_{2u}; ip)	1450 (1326; 1573; +247)	1435(+), 1454(−) (9; 0.6 %)	–15, +4 (−1.0 %, 0.3 %)
ν_{19} (e_{1u}; ip)	1453 (1486; 1420; −66)	1449(+), 1453(−) (4; 0.3 %)	–4, 0 (−0.3 %, 0 %)
ν_{8}	1616	1541(–), 1615(+)	−76, −1

(e_{2g}; ip)	(1649; 1583; −66)	(74; 4.7 %)	(−4.7 %, −0.1 %)
v_{13} (b_{2u}; ip)	3052 (3039; 3064; +25)	3047(–),3048(+) (1; 0.0 %)	−5, −4 (−0.2 %, −0.1 %)
v_7 (e_{2g}; ip)	3058 (3048; 3068; +20)	3052(+),3055(−) (3; 0.1 %)	−6, −3 (−0.2 %, −0.1 %)
v_{20} (e_{1u}; ip)	3074 (3063; 3084; +21)	3070(−),3071(+) (1; 0.0 %)	−4, −3 (−0.1 %, −0.1 %)
v_2 (a_{1g}; ip)	3083 (3072; 3094; +22)	3076(−),3082(+) (6; 0.2 %)	−7, −1 (−0.2 %, −0.0 %)

Table S4 Theoretical (ν_{calc}) vibrational frequencies and the assignments of Bz and Bz_2 in the S_0 and S_1 states calculated by normal mode analyses on the optimized structures obtained by CAM-B3LYP/aug-cc-pVTZ and TD-CAM-B3LYP/aug-cc-pVTZ level of theory with GD3BJ empirical dispersion correction, respectively.

a) These are scaled values by 0.98 for skeletal vibrations and 0.95 for CH stretching vibrations, respectively. Values in parentheses are transition intensities in km/mol.

b) +/− on the shoulder means the signs of the linear combinations, see text. Symmetry species in the D_{6h} point group are denoted in parentheses.

Bz (S_0)		Bz (S_1)		Bz_2 (S_1, SW, D_{6h})		Bz_2 (S_1, T, C_{2v})	
ν_{calc} / cm^{-1} a)	assignments b)	ν_{calc} / cm^{-1} a)	assignments	ν_{calc} / cm^{-1} a)	assignments b)	ν_{calc} / cm^{-1} a)	assignments
				64 (0)	R_z	−23 (0)	R_x
				118 (0)	$\beta_{(x, y)}$	11 (0)	R_y
				118 (0)	$\beta_{(x, y)}$	41(0)	R_z
				132 (1)	$R_{(x, y)}$	53 (0)	σ_z
				132 (1)	$R_{(x, y)}$	61 (0)	β_x
				154 (0)	σ_z	62 (0)	β_y
410 (0)	16 (e_{2u})	246 (0)	16 (e_{2u})	359 (0)	16^- (e_{2g})	244 (0)	16a (stem)
				382 (0)	16^+ (e_{2u})	247 (0)	16b (stem)
		340 (0)	4 (b_{2g})			346 (0)	4 (stem)
						410 (0)	16b (top)
617 (0)	6 (e_{2g})			534 (0)	6^+ (e_{2g})	410 (0)	16a (top)
		524 (0)	6 (e_{2g})	592 (0)	6^- (e_{2u})	520 (0)	6b (stem)
						529 (0)	6a (stem)
						562 (120)	11 (stem)
718 (0)	4 (b_{2g})			598 (0)	4^- (b_{1u})	617 (0)	6b (top)
				616 (0)	4^+ (b_{2g})	617(0)	6a (top)
688 (113)	11 (a_{2u})	562 (147)	11 (a_{2u})	643 (117)	11^+ (a_{2u})	624 (0)	10a (stem)
				675 (0)	11^- (a_{1g})	624 (0)	10b (stem)
868 (0)	10 (e_{1g})	623 (0)	10 (e_{1g})	778 (0)	10^+ (e_{1g})	689 (126)	11 (top)
				774 (4)	10^- (e_{1u})	723 (0)	4 (top)
						773 (0)	17a (stem)
						796 (0)	17b (stem)
997 (0)	17 (e_{2u})	778 (0)	17 (e_{2u})	897 (0)	17^- (e_{2g})	826 (0)	5 (stem)
				906 (0)	17^+ (e_{2u})	870 (0)	10b (top)
						870 (0)	10a (top)
						960 (1)	1 (stem)
1023 (0)	5 (b_{2g})	811 (0)	5 (b_{2g})	920 (0)	5^- (b_{1u})	978 (2)	18a (stem)
				934 (0)	5^+ (b_{2g})	979 (5)	18b (stem)
1015 (0)	1 (a_{1g})	961 (0)	1 (a_{1g})	910 (50)	1^- (a_{2u})	1000 (1)	12 (stem)

1020 (0)	12 (b_{1u})	1000 (0)	12 (b_{1u})	1012 (0)	12^{-} (b_{2g})	1000 (0)	17a (top)
				1012 (0)	12^{+} (b_{1u})	1001 (0)	17b (top)
				994 (0)	1^{+} (a_{1g})	1012 (0)	1 (top)
1054 (11)	18 (e_{1u})	979 (9)	18 (e_{1u})	1018 (6)	18^{+} (e_{1u})	1020 (0)	12 (top)
				1023 (0)	18^{-} (e_{1g})	1029 (0)	5 (top)
						1054 (5)	18b (top)
						1054 (4)	18a (top)
1150 (0)	15 (b_{2u})	1159 (0)	15 (b_{2u})	1160 (0)	15^{-} (b_{1g})	1152 (0)	15 (top)
				1161 (0)	15^{+} (b_{2u})	11572 (1)	15 (stem)
1182 (0)	9 (e_{2g})	1163 (0)	9 (e_{2g})	1153 (0)	9^{-} (e_{2u})	1161 (1)	9a (stem)
				1175 (0)	9^{+} (e_{2g})	1164 (1)	9b (stem)
						1183 (0)	9a (top)
						1183 (0)	9b (top)
1370 (0)	3 (a_{2g})	1351 (0)	3 (a_{2g})	1359 (0)	3^{-} (a_{1u})	1307 (0)	14 (top)
				1360 (0)	3^{+} (a_{2g})	1351 (0)	3 (stem)
1306 (0)	14 (b_{2u})	1538 (0)	14 (b_{2u})	1414 (0)	14^{+} (b_{2u})	1371 (0)	3 (top)
1504 (15)	19 (e_{1u})	1442 (8)	19 (e_{1u})	1472 (16)	19^{+} (e_{1u})	1440 (6)	19a (stem)
				1474 (0)	19^{-} (e_{1g})	1442 (2)	19b (stem)
						1505 (9)	19a (top)
						1505 (8)	19b (top)
				1428 (0)	14^{-} (b_{1g})	1536 (1)	14 (stem)
1638 (0)	8 (e_{2g})	1571 (0)	8 (e_{2g})	1542 (0)	8^{-} (e_{2u})	1570 (0)	8b (stem)
				1609 (0)	8^{+} (e_{2g})	1570 (0)	8a (stem)
						1636 (0)	8b (top)
						1636 (1)	8a (top)
3022 (0)	13 (b_{1u})	3049 (0)	13 (b_{1u})	3036 (0)	13^{-} (b_{2g})	3025 (0)	13 (top)
				3037 (0)	13^{+} (b_{1u})	3033 (0)	7b (top)
3032 (0)	7 (e_{2g})	3054 (0)	7 (e_{2g})	3043 (0)	7^{+} (e_{2g})	3034 (0)	7a (top)
				3044 (0)	7^{-} (e_{2u})	3048 (19)	20b (top)
						3048 (0)	13 (stem)
						3049 (20)	20a (top)
3046 (54)	20 (e_{1u})	3069 (27)	20 (e_{1u})	3057 (0)	20^{-} (e_{1g})	3052 (0)	7b (stem)
				3059 (30)	20^{+} (e_{1u})	3057 (0)	2 (top)
						3059 (11)	7a (stem)
						3067 (14)	20b (stem)
3056 (0)	2 (a_{1g})	3079 (0)	2 (a_{1g})	3063 (28)	2^{-} (a_{2u})	3074 (2)	2 (stem)
				3070 (0)	2^{+} (a_{1g})	3100 (4)	20a (stem)

Table S5 Comparison between theoretical average frequencies of the S_0 and S_1 states (ν_{ave}) and the EXC state (ν_{EXC}) calculated at CAM-B3LYP/aug-cc-pVTZ and TD-CAM-B3LYP/aug-cc-pVTZ level of theory with GD3BJ empirical dispersion correction, respectively. The second column lists frequencies in the EXC state, ν_{EXC}, and absolute values of splitting of the modes, $|\Delta\nu_{EXC}(+/-)| = |\nu_{EXC}(+) - \nu_{EXC}(-)|$, and percentage of the splitting to the average frequencies $\langle\nu_{EXC}\rangle = (\nu_{EXC}(+) + \nu_{EXC}(-))/2$. The third column shows deviations from the average values ($\Delta\nu = \nu_{EXC} - \nu_{ave}$) and percentages of difference to the average values.

Mode	ν_{ave} / cm^{-1} ($\nu(S_0)$; $\nu(S_1)$; $\Delta\nu(S_1/S_0)$)	ν_{EXC} / cm^{-1} ($|\Delta\nu_{EXC}(+/-)|$; $|\Delta\nu_{EXC}(+/-)|/\langle\nu_{EXC}\rangle$)	$\Delta\nu$ / cm^{-1} ($\Delta\nu$ / ν_{ave})
ν_{16} (e_{2u}; op)	331 (410; 246; −163)	359 (−), 382 (+) (23; 6.2 %)	+29, +52 (+8.8 %, +15.7 %)
ν_{6} (e_{2g}; ip)	570 (617; 523; −93)	534 (+), 592 (−) (59; 10.4 %)	−37, +22 (−6.4 %, +3.9 %)
ν_{4} (b_{2g}; op)	529 (718; 340; −378)	598 (−), 616 (+) (18; 3.0 %)	+69, +87 (+13.0 %, +16.4 %)
ν_{11} (a_{2u}; op)	625 (688; 562; −126)	643 (+), 675 (−) (32; 4.8 %)	+18, +50 (+3.0 %, +8.1 %)
ν_{10} (e_{1g}; op)	746 (868; 623; −246)	778 (+), 774 (−) (5; 0.6 %)	+33, +28 (+4.4 %, +3.8 %)
ν_{17} (e_{2u}; op)	888 (997; 778; −219)	897 (−), 906 (+) (9; 1.0 %)	+10, +18 (+1.1 %, +2.1 %)
ν_{5} (b_{2g}; op)	917 (1023; 811; −211)	920 (−), 934 (+) (14; 1.5 %)	+3, +17 (+0.3 %, +1.8 %)
ν_{1} (a_{1g}; ip)	988 (1015; 961; −54)	910 (−), 994 (+) (83; 8.8 %)	−78, +6 (−7.9 %, +0.6 %)
ν_{12} (b_{1u}; ip)	1010 (1020; 1000; −20)	1012 (−), 1012 (+) (0; 0.0 %)	+2, +3 (+0.2 %, +0.3 %)
ν_{18} (e_{1u}; ip)	1016 (1054; 979; −75)	1018 (+), 1023 (−) (5; 0.4 %)	+2, +7 (+0.2 %, +0.7 %)
ν_{15} (b_{2u}; ip)	1155 (1150; 1159; +9)	1160 (−), 1161 (+) (1; 0.1 %)	+5, +6 (+0.4 %, +0.5 %)
ν_{9} (e_{2g}; ip)	1173 (1182; 1163; −19)	1153 (−), 1175 (+) (22; 1.9 %)	−20, +2 (−1.7 %, +0.2 %)
ν_{3} (a_{2g}; ip)	1361 (1370; 1351; −19)	1359 (−), 1360 (+) (1; 0.1 %)	−1, −0 (−0.1 %, −0.0 %)
ν_{14} (b_{2u}; ip)	1422 (1306; 1538; +232)	1414 (+), 1428 (−) (13.89; 0.98 %)	–8, +6 (−0.5 %, +0.4 %)
ν_{19} (e_{1u}; ip)	1473 (1504; 1442; −62)	1472 (+), 1474 (−) (2; 0.2 %)	–1, +1 (−0.1 %, +0.1 %)
ν_{8}	1605	1542 (–), 1609 (+)	−63, +4

(e_{2g}; ip)	(1638; 1571; −67)	(67; 4 %)	(−3.9 %, +0.2 %)
v_{13} (b_{2u}; ip)	3036 (3022; 3049; +27)	3036 (–), 3037 (+) (1; 0.1 %)	+0, +2 (+0.0 %, +0.1 %)
v_7 (e_{2g}; ip)	3043 (3032; 3054; +22)	3043 (+), 3044 (−) (1; 0.0 %)	−0, −1 (−0.0 %, −0.0 %)
v_{20} (e_{1u}; ip)	3058 (3046; 3069; +22)	3057 (−), 3059 (+) (2; 0.1 %)	−0, +2 (−0.0 %, +0.1 %)
v_2 (a_{1g}; ip)	3067 (3056; 3079; +23)	3063 (−), 3070 (+) (6; 0.2 %)	−4, +2 (−0.1 %, +0.1 %)

Table S6 Comparison between average frequencies in the S_0 and S_1 states (ν_{ave}) and those in the EXC state (ν_{EXC}). Difference of these values ($\Delta\nu = \nu_{EXC} - \nu_{ave}$) are listed in the third column. Calculated values obtained by CAM-B3LYP/aug-cc-pVTZ and TD-CAM-B3LYP/aug-cc-pVTZ levels of theory with GD3BJ empirical dispersion correction are shown below the experimental values. Two IR active modes are possible for combination modes from degenerate species, see text.

[a] Deperturbed values taken from ref. 84 and ref. 87.

Mode		ν_{ave} / cm^{-1} (S_0; $S_1 6^1$)	ν_{EXC} / cm^{-1} (FWHM / cm^{-1})	$\Delta\nu$ / cm^{-1} ($\Delta\nu$ / ν_{ave})
ν_{18} (in plane)	Obs	980 (1040; 920)	989 (12)	+9 (+0.9 %)
	Calc	1016 (1054; 979; −75)	1018	+2 (+0.2 %)
$\nu_5 + \nu_{16}$ (out-of-plane)	Obs	– (1390; –)	– (–)	– (–)
	Calc	1245 (1433; 1053)	1280, 1317	+34, +71 (+2.8 %, +5.7 %)
$\nu_{10} + \nu_{11}$ (out-of-plane)	Obs	1308 (1519; 1096)	1340 (~60)	+32 (+2.4 %)
	Calc	1370 (1556; 1185)	1421, 1449	+51, +78 (+3.7 %, +5.7 %)
ν_{19} (in plane)	Obs	1444 (1485; 1402)	1439 (9)	−5 (−0.3 %)
	Calc	1473 (1504; 1442)	1472	–1 (−0.1 %)
$\nu_{10} + \nu_{17}$ (out-of-plane)	Obs	1557 (1814; 1300)	1570 (~80)	+13 (+0.8 %)
	Calc	1633 (1865; 1401)	1671, 1684	+37, +51 (+2.3 %, +3.1 %)
$\nu_5 + \nu_{17}$ (out-of-plane)	Obs	1713 (1960; 1465)	1700 (~60)	−13 (−0.6 %)
	Calc	1805 (2020; 1590)	1817, 1840	+12, +35 (+0.7 %, +2.0 %)
ν_{20} (in plane)	Obs	3072 (3065; 3079)[a]	3075 (6)	+3 (+0.1 %)
	Calc	3057 (3046; 3069)	3059	+2 (+0.1 %)

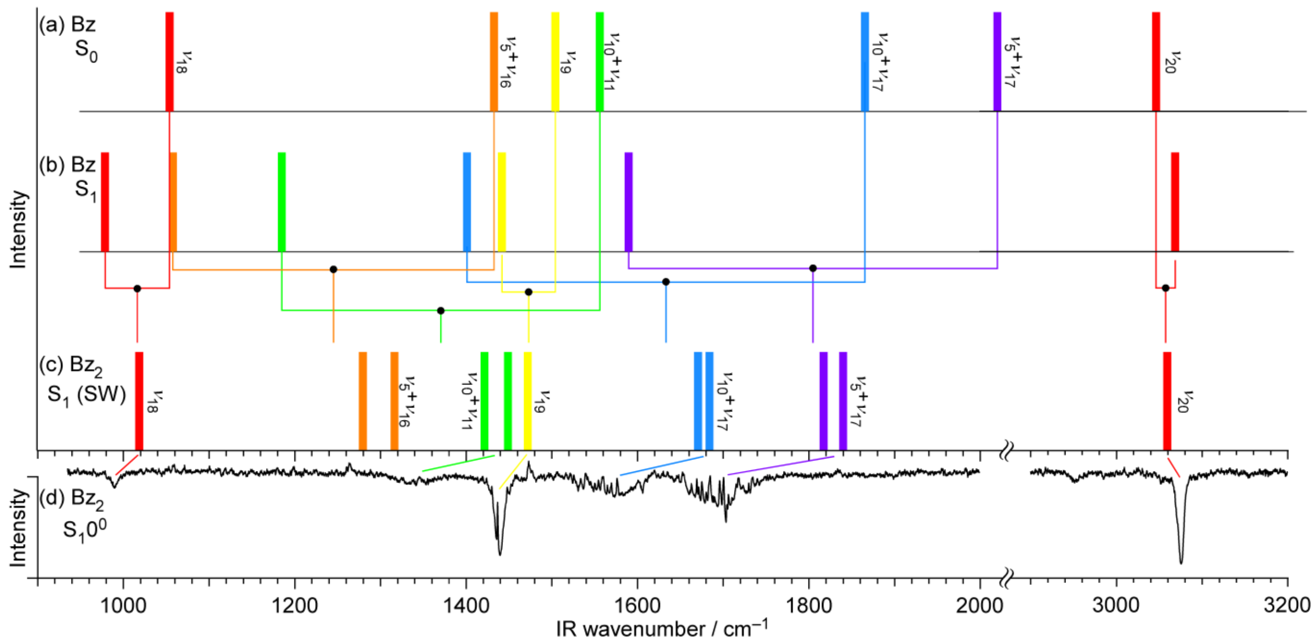

Figure S2 Comparison of vibration frequencies of (a) Bz in S_0, (b) Bz in S_1 and (c) Bz_2 in S_1 states (SW structure) obtained by CAM-B3LYP/aug-cc-pVTZ and TD-CAM-B3LYP/aug-cc-pVTZ levels of theory with the GD3BJ empirical dispersion correction, and the experimental spectrum (d). Positions of the combination bands are calculated as simple sums of the respective fundamental frequencies. Black circles indicate the average positions of the vibration frequencies in the S_0 and S_1 states of Bz. Vertical lines drown from the circles compare the average positions with frequencies calculated for the SW EXC state. In the panel (c), two bars with the same color show positions of two different IR active combinations, see the main text. This is a figure corresponding to Figure 5 in the main text but with the CAM-B3LYP functional.

The full expression of the excimer state vibrational energy, $E_{v_\pm}^{+/-\,\prime}$, derived from the secular determinant given by equation (33) in Appendix.

Since the secular determinant derives a quadratic equation, the solution is written in the standard form:

$$E_{v_\pm}^{+/-\,\prime} = \frac{B +/- \sqrt{C}}{2A}. \tag{S1}$$

Here, factors *A*, *B*, and *C* are expressed as follows (notation of factors follows that in ***Appendix***):

$$A = \left\{1 \pm \langle S\rangle \langle FC_{0^*v}^{\phi}\rangle^2 \boldsymbol{FC}_{0^*0}{}^2\right\}\left\{1 \pm \langle S\rangle \langle FC_{v^*0}^{\phi}\rangle^2 \boldsymbol{FC}_{0^*0}{}^2\right\} - \langle S\rangle^2 \langle FC_{v^*0}^{\phi}\rangle^2 \boldsymbol{FC}_{0^*0}{}^4$$

$$= 1 \pm \langle S\rangle \left(\langle FC_{0^*v}^{\phi}\rangle^2 + \langle FC_{v^*0}^{\phi}\rangle^2\right) \boldsymbol{FC}_{0^*0}{}^2 + \langle S\rangle^2 \left(\langle FC_{0^*v}^{\phi}\rangle^2 \langle FC_{v^*0}^{\phi}\rangle^2 - \langle FC_{v^*v}^{\phi}\rangle^2\right) \boldsymbol{FC}_{0^*0}{}^4, \tag{S2}$$

$$B = \left\{1 \pm \langle S\rangle \langle FC_{v^*0}^{\phi}\rangle^2 \boldsymbol{FC}_{0^*0}{}^2\right\}\left\{h\nu \pm (\langle EXC\rangle + 2\langle S\rangle\langle T_{0^*v}\rangle) \langle FC_{0^*v}^{\phi}\rangle^2 \boldsymbol{FC}_{0^*0}{}^2\right\}$$

$$+\left\{1 \pm \langle S\rangle \langle FC_{0^*v}^{\phi}\rangle^2 \boldsymbol{FC}_{0^*0}{}^2\right\}\left\{h\nu^* \pm (\langle EXC\rangle + 2\langle S\rangle\langle T_{v^*0}\rangle) \langle FC_{v^*0}^{\phi}\rangle^2 \boldsymbol{FC}_{0^*0}{}^2\right\}$$

$$-2\langle S\rangle(\langle EXC\rangle + \langle S\rangle\langle T_{v^*v}\rangle) \langle FC_{v^*0}^{\phi}\rangle^2 \boldsymbol{FC}_{0^*0}{}^4$$

$$= h\nu + h\nu^* \pm \Big((\langle EXC\rangle + 2\langle S\rangle\langle T_{0^*v}\rangle) \langle FC_{0^*v}^{\phi}\rangle^2 + (\langle EXC\rangle + 2\langle S\rangle\langle T_{v^*0}\rangle) \langle FC_{v^*0}^{\phi}\rangle^2 + \langle S\rangle \left(\langle FC_{0^*v}^{\phi}\rangle^2 h\nu^* + \langle FC_{v^*0}^{\phi}\rangle^2 h\nu\right)\Big) \boldsymbol{FC}_{0^*0}{}^2 +$$

$$2\langle S\rangle \left(\left(\langle EXC\rangle + \langle S\rangle(\langle T_{0^*v}\rangle + \langle T_{v^*0}\rangle)\right) \langle FC_{0^*v}^{\phi}\rangle^2 \langle FC_{v^*0}^{\phi}\rangle^2 - (\langle EXC\rangle + \langle S\rangle\langle T_{v^*v}\rangle) \langle FC_{v^*v}^{\phi}\rangle^2\right) \boldsymbol{FC}_{0^*0}{}^4, \tag{S3}$$

$$C =$$

$$\Big[\left\{1 \pm \langle S\rangle \langle FC_{v^*0}^{\phi}\rangle^2 \boldsymbol{FC}_{0^*0}{}^2\right\}\left\{h\nu \pm (\langle EXC\rangle + 2\langle S\rangle\langle T_{0^*v}\rangle) \langle FC_{0^*v}^{\phi}\rangle^2 \boldsymbol{FC}_{0^*0}{}^2\right\} -$$

$$\left\{1 \pm \langle S\rangle \langle FC_{0^*v}^{\phi}\rangle^2 \boldsymbol{FC}_{0^*0}{}^2\right\}\left\{h\nu^* \pm (\langle EXC\rangle + 2\langle S\rangle\langle T_{v^*0}\rangle) \langle FC_{v^*0}^{\phi}\rangle^2 \boldsymbol{FC}_{0^*0}{}^2\right\}\Big]^2 + 4 \langle FC_{v^*v}^{\phi}\rangle^2 \boldsymbol{FC}_{\boldsymbol{0}^*\boldsymbol{0}}{}^4 \Big[\{\langle S\rangle h\nu -$$

$$(\langle EXC\rangle + \langle S\rangle\langle T_{v^*v}\rangle)\} \pm \langle S\rangle^2 (2\langle T_{0^*v}\rangle - \langle T_{v^*v}\rangle) \langle FC_{0^*v}^{\phi}\rangle^2 \boldsymbol{FC}_{0^*0}{}^2\Big]\Big[\{\langle S\rangle h\nu^* - (\langle EXC\rangle + \langle S\rangle\langle T_{v^*v}\rangle)\} \pm$$

$$\langle S\rangle^2 (2\langle T_{v^*0}\rangle - \langle T_{v^*v}\rangle) \langle FC_{v^*0}^{\phi}\rangle^2 \boldsymbol{FC}_{0^*0}{}^2\Big]. \tag{S4}$$

In the case of a non-totally symmetric mode, two FC factors vanish due to a requirement of the symmetry, $\langle FC_{0^*v}^{\phi}\rangle = \langle FC_{v^*0}^{\phi}\rangle = 0$. This condition reduces the above terms as follows:

$$A = 1 - \langle S\rangle^2 \langle FC_{v^*v}^{\phi}\rangle^2 \boldsymbol{FC}_{0^*0}{}^4, \tag{S2′}$$

$$B = h\nu + h\nu^* - 2\langle S\rangle(\langle EXC\rangle + \langle S\rangle\langle T_{v^*v}\rangle) \langle FC_{v^*v}^{\phi}\rangle^2 \boldsymbol{FC}_{0^*0}{}^4, \tag{S3′}$$

$$C = (h\nu - h\nu^*)^2 + 4\langle FC^{\phi}_{\nu^*\nu}\rangle^2 \boldsymbol{FC}_{0^*0}{}^4\{\langle S\rangle h\nu - (\langle EXC\rangle + \langle S\rangle\langle T_{\nu^*\nu}\rangle)\}\{\langle S\rangle h\nu^* - (\langle EXC\rangle + \langle S\rangle\langle T_{\nu^*\nu}\rangle)\}$$

$$= \left\{1 - \langle S\rangle^2 \langle FC^{\phi}_{\nu^*\nu}\rangle^2 \boldsymbol{FC}_{0^*0}{}^4\right\}(h\nu - h\nu^*)^2 + \{2(\langle EXC\rangle + \langle S\rangle\langle T_{\nu^*\nu}\rangle) - \langle S\rangle(h\nu + h\nu^*)\}^2 \langle FC^{\phi}_{\nu^*\nu}\rangle^2 \boldsymbol{FC}_{0^*0}{}^4. \tag{S4'}$$

The first term of equation (S4′) is considered to be much smaller than the second term because of a factor of vibrational energy difference. Thus, square root of equation (S4′) can be expanded as follows:

$$\sqrt{C} = \{2(\langle EXC\rangle + \langle S\rangle\langle T_{\nu^*\nu}\rangle) - \langle S\rangle(h\nu + h\nu^*)\}\langle FC^{\phi}_{\nu^*\nu}\rangle \boldsymbol{FC}_{0^*0}{}^2 \left(1 + \frac{\left\{1-\langle S\rangle^2\langle FC^{\phi}_{\nu^*\nu}\rangle^2\boldsymbol{FC}_{0^*0}{}^4\right\}(h\nu-h\nu^*)^2}{\{2(\langle EXC\rangle+\langle S\rangle\langle T_{\nu^*\nu}\rangle)-\langle S\rangle(h\nu+h\nu^*)\}^2\langle FC^{\phi}_{\nu^*\nu}\rangle^2\boldsymbol{FC}_{0^*0}{}^4}\right)^{\frac{1}{2}}$$

$$\approx \{2(\langle EXC\rangle + \langle S\rangle\langle T_{\nu^*\nu}\rangle) - \langle S\rangle(h\nu + h\nu^*)\}\langle FC^{\phi}_{\nu^*\nu}\rangle \boldsymbol{FC}_{0^*0}{}^2 + \frac{1}{2}\frac{\left\{1-\langle S\rangle^2\langle FC^{\phi}_{\nu^*\nu}\rangle^2\boldsymbol{FC}_{0^*0}{}^4\right\}(h\nu-h\nu^*)^2}{\{2(\langle EXC\rangle+\langle S\rangle\langle T_{\nu^*\nu}\rangle)-\langle S\rangle(h\nu+h\nu^*)\}\langle FC^{\phi}_{\nu^*\nu}\rangle\boldsymbol{FC}_{0^*0}{}^2}. \tag{S5'}$$

Then, the expression of $E^{+/-\prime}_{\nu_\pm}$, which is used in the appendix as equation (36), can be obtained by substituting equation (S2′)–(S5′) into (S1).

$$E^{+/-\prime}_{\nu_\pm} \approx \frac{(h\nu+h\nu^*)}{2\left(1{+/-}\langle S\rangle\langle FC^{\phi}_{\nu^*\nu}\rangle\boldsymbol{FC}_{0^*0}{}^2\right)} {+/-} \frac{(\langle EXC\rangle+\langle S\rangle\langle T_{\nu^*\nu}\rangle)\langle FC^{\phi}_{\nu^*\nu}\rangle\boldsymbol{FC}_{0^*0}{}^2}{\left(1{+/-}\langle S\rangle\langle FC^{\phi}_{\nu^*\nu}\rangle\boldsymbol{FC}_{0^*0}{}^2\right)} {+/-} \frac{(h\nu-h\nu^*)^2}{4\{2\langle EXC\rangle+2\langle S\rangle\langle T_{\nu^*\nu}\rangle-\langle S\rangle(h\nu+h\nu^*)\}\langle FC^{\phi}_{\nu^*\nu}\rangle\boldsymbol{FC}_{0^*0}{}^2} \tag{S6}$$